

INTERNATIONAL SOCIETY FOR SOIL MECHANICS AND GEOTECHNICAL ENGINEERING



This paper was downloaded from the Online Library of the International Society for Soil Mechanics and Geotechnical Engineering (ISSMGE). The library is available here:

<https://www.issmge.org/publications/online-library>

This is an open-access database that archives thousands of papers published under the Auspices of the ISSMGE and maintained by the Innovation and Development Committee of ISSMGE.

The paper was published in the proceedings of the 10th International Conference on Physical Modelling in Geotechnics and was edited by Moonkyung Chung, Sung-Ryul Kim, Nam-Ryong Kim, Tae-Hyuk Kwon, Heon-Joon Park, Seong-Bae Jo and Jae-Hyun Kim. The conference was held in Daejeon, South Korea from September 19th to September 23rd 2022.

Utilising point clouds to characterize defect sets in rock slopes

K. Stariha & H. Baxter-Crawford
SMEC Australia Pty Ltd, Australia

ABSTRACT: As remote sensing technology has improved, advances have been made in using new forms of data to remotely undertake slope stability analysis. This is particularly useful where slopes may be difficult or unsafe to access. This paper outlines the processing and analysis of a point cloud collected at three outcrops adjacent to Bendora Dam which are no longer deemed safe to access. Analysis of the point cloud was undertaken to visualize existing defect sets and to characterize their orientation, spacing and waviness. An analysis of point normal orientation was undertaken to assess a directionally dependent dilation angle along exposed bedding surfaces.

Keywords: remote sensing, point cloud, dilation angle, defect characterisation

1 INTRODUCTION

1.1 Remote Sensing

Remote sensing is the process of obtaining information about an area without contacting said area. This can be particularly useful in rock slope engineering, where physical access to slopes may be limited due to safety concerns. Forms of remote sensing most regularly adopted for geological/geotechnical projects include LiDAR and photogrammetry.

Remote sensing data may be presented either as point clouds or meshed surfaces (Gigli & Casagli, 2011). International trends in remote sensing analysis (Turner et al., 2006, Dong et al., 2020) are now leaning towards the direct extraction of features from point clouds, rather than from derivative surfaces such as meshes. In a point cloud, each data point contains an individual x, y, and z coordinate. It is standard practice to combine data from multiple scans in order to improve accuracy and to prevent any shadowing of features which may occur from any one measurement location and diurnal influences.

1.2 Study Area

Bendora Dam is a 47m high double curvature variable arch dam located on the Cotter River in the Australian Capital Territory (ACT) of Australia. It is located in a narrow V-shaped gorge (some 25 m wide) defined by outcrops of the Tidbinbilla Quartzite. The geology of the site is detailed in companion paper, Baxter-Crawford and Stariha- (2022).

As input to a 20-year Dam Safety Review, a remote sensing survey was taken of three rock outcrops, two on the right abutment, one on the left (Fig. 1). Whilst these outcrops were mapped traditionally by hand in the 1950's to the early 2000's, safety guidelines at Bendora Dam now mean that access to these abutments is only

permitted with 'safe rope work' procedures. This makes the site a perfect candidate for remote sensing analysis. The database collated was used to assess the structural orientation, spacing and surface character of defect sets at the dam.



Fig. 1: Location of three outcrops under investigation.

2 DATA COLLECTION

Data was collected using both photogrammetry and LiDAR scanning. UAV photogrammetry was undertaken with a DJI Phantom 4 Pro Mk2 drone, with a 20 mega pixel camera. Ground control targets were used to ensure accuracy, and multiple flights were completed to achieve full coverage of the target areas. Captured photographs were georeferenced and processed to develop a 3D point cloud. Terrestrial (ground based) LiDAR was undertaken to enhance the accuracy of coverage where accessible.

Data from these two sources were combined and processed for noise before being provided as a rendered

point cloud, with an approximate grid resolution of 0.058 m and accuracy of 20 mm horizontally, and 50 mm vertically. Fig. 2 below displays the lower outcrop on the right abutment, comparing a photograph to the rendered point cloud.



Fig. 2: Comparison of the outcrop on the right abutment a) as a photograph (November 2020); and b) as a screenshot of the point cloud generated from remote sensing (January 2020), presented in CloudCompare.

3 DATA PROCESSING

The open source program CloudCompare (V2.12α) was used to display and process the rendered point cloud. CloudCompare contains several purpose-built plugins and algorithms which allow for specialist measurements and data processing applications, including a structural geology toolbox called Compass.

3.1 Orientation

The Compass tool was used to manually capture orientation measurements from the rendered point cloud. Measurement locations were judged to be representative of exposed defect surfaces and were taken on a range of large and small planes. Where defects had an apparent waviness, the measurement plane was extended to take an average orientation across the surface. The compass tool generated a numerical list of measurement information (dip and dip direction) which was imported into the program DIPS by RocScience.

Three sub-vertical joint sets and one bedding set were observed in each of the three outcrops, as displayed below. The orientation of sets are graphically defined in

Fig. 3, and numerically in Table 1.

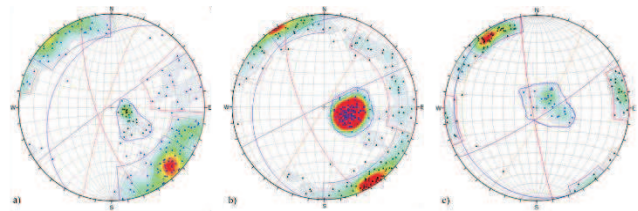


Fig. 3: Graphical representation of defect orientation in outcrops a) Upper right; b) Lower right; c) Left

Table 1: Summary of defect set orientation from remote sensing data – Dip and Dip Direction (True North)

Abutment Set	Upper Right		Lower Right		Left	
	Dip	Dip Dir.	Dip	Dip Dir.	Dip	Dip Dir.
Joint Set 1	71	251	71	246	86	260
Joint Set 2	87	324	88	334	82	148
Joint Set 3	82	288	90	122.	83	120
Bedding	25	299	24	284	12	251

3.2 Set Segregation and Visualization

To assist the analysis of spacing and surface character, the point cloud was segmented into separate point clouds for each defect set. CloudCompare can analyse a point cloud using vector statistical considerations, using the relationship of a point to its’ neighbours to define the normal orientation of each point. A Hough Normal transformation was chosen, which is robust to noise, outliers, density variation and sharp edges.

The qFacets plugin in CloudCompare was used to segregate the point cloud on the basis of point orientation, using the outer limits of the measured set orientation ranges for segmentation. The point cloud for each set was assigned a solid colour, corresponding to the colours in Table 1. This aided in visualizing the relationships between defect sets and topography. An example of the segmented point cloud is presented as an overlay on the rendered true colour point cloud, in Fig. 4 and Fig. 5 for the left and right abutments respectively.

The outcrop can be observed to be blocky in nature, with clear “moulds” observed from which joint-defined blocks have failed.

3.3 Set Normal Spacing

Set normal spacing is the measurement of the true distance between two defects in the same set, normal to the plane’s orientation. This determines the shape and volume of rock blocks which, when compared to the geometry of an excavation or slope face, may impact overall slope stability.

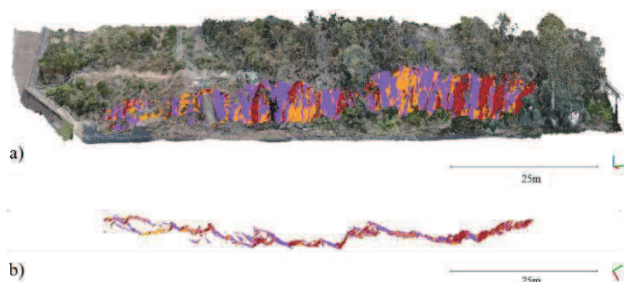


Fig. 4: Left Abutment, looking north-west; a) true colour point cloud overlain with coloured defect sets, looking horizontally; and b) coloured defect sets, looking vertically.

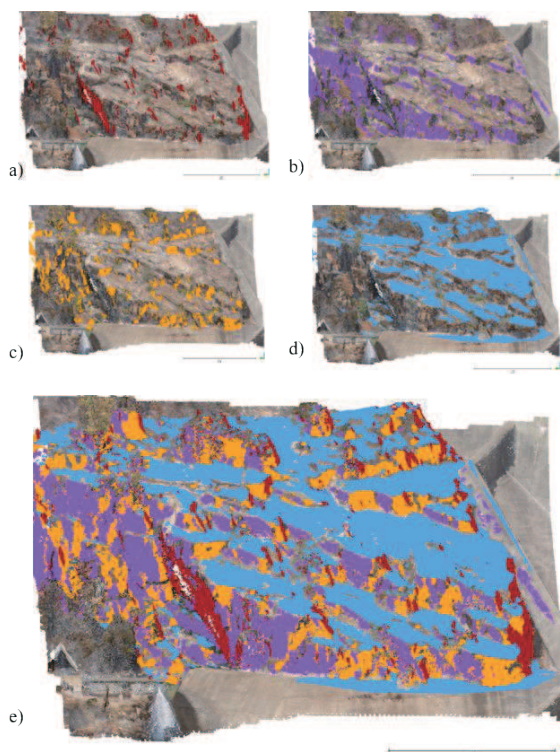


Fig. 5: Lower Right Abutment - Solid colour overlay for each of the defect sets on the true colour point cloud, inclined looking south-east; a) Joint Set 1 (red); b) Joint Set 2 (purple); c) Joint Set 3 (orange); d) Bedding (blue); and e) All defect sets

In outcrop, it is not always possible to observe a structural set at the appropriate angle to measure the true spacing. The CloudCompare ‘Compass’ plug-in contains a “2-point thickness” tool, which is able to measure the distance between two points with a defined orientation of measurement. By setting the orientation of measurement to the mean set orientation, it is possible to directly measure the spacing in this direction. Fig. 6 presents an example of the spacing measurement process for bedding in the Lower Right outcrop. The results were commensurate with field mapping, between 1-1.4 m for bedding partings, 1.2-3.2 m for Joint Set 1, 0.7-2.8 m for Joint Set 2, and 2.0-2.8 m for Joint Set 3.

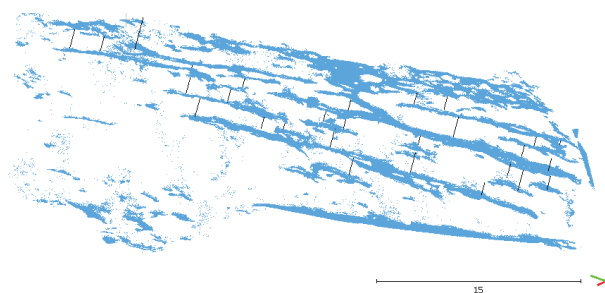


Fig. 6: Measurement of spacing (black) between bedding planes (blue).

3.4 Surface Character

The surface character of a defect affects the mechanical behaviour of a rock mass by influencing the shear strength of a defect surface. There are two distinct components of surface roughness:

- First order: Large scale waviness, occurring at a scale of > 500 mm; and
- Second order: Small-scale unevenness/roughness, occurring at a scale of 10-100 mm.

Surface roughness provides a shear resistance to movement which is typically described through a mobilised friction angle. The mobilised friction angle comprises a basic friction angle (ϕ_b) and a dilation angle (i). The dilation angle (i) represents the angle at which dilation will occur if shear movement is applied to a joint surface, including the waviness and roughness of a surface. The dilation angle is measured from the mean defect plane.

In CloudCompare, it is possible to define both the dilation angle, and the amplitude of waviness along a defect surface from the mean defect plane. Taken over an appropriate (block-size) interval, this provides information as to the resistance to movement for each block along that defect surface. The dilation angle and waviness amplitude were measured for bedding only, on the Lower Right abutment which had clearly exposed bedding planes. Measurements were undertaken over areas between 1 m² and 2.5 m², in line with the measured joint spacing. Considering areas larger than this would take into account any larger scale defect waviness, which may not have an impact on the block scale.

Waviness Amplitude

Quantitatively, waviness in the field is most typically measured by placing a straight edge on an exposed joint plane and measuring the maximum surface offset/amplitude at intervals along this edge. This method can be adapted to 3D point clouds, by measuring the offset of a defect surface from a mean plane. The proposed 3D method analyses an area rather than a line. It is therefore considered a more appropriate reflection of the movement of a block along a surface, recognising that the whole block will dilate over an asperity.

This procedure was undertaken using the “Compass” tool in Cloud Compare to define a mean plane of best fit. The “1 point thickness” measuring tool was then used to measure offset from that mean plane to the furthest points comprising the defect surface. The offset was measured to either side of the mean plane, and the amplitude was defined as an average between the offset above and below the mean plane, Fig. 7. The mean waviness amplitude for bedding surfaces was 300 mm, with a standard deviation of 100 mm, across test areas of between 1 m² and 2.5 m².

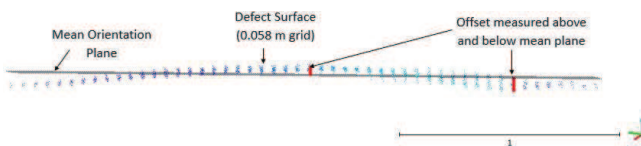


Fig. 7: Measurement of maximum waviness amplitude, bedding plane 1, viewed along strike.

Dilation Angle

As new technology relating to remote sensing has been developed, new methodologies for deriving the dilation angle from point clouds have arisen. Dong et al. (2020) suggested a method of calculating the dilation angle from high resolution point cloud data. By calculating the normal orientation of each point within the point cloud, it is possible to define any variation in orientation from the mean plane.

Variation in orientation is best measured by plotting the orientation of point-normals on an equal area stereonet and defining the dilation angle as the scatter of normal from the cone axis (mean bedding plane). Dilation angles were measured from the 3D point cloud for 10 bedding surfaces on the Lower Right abutment. An example is included in Fig. 8 below.

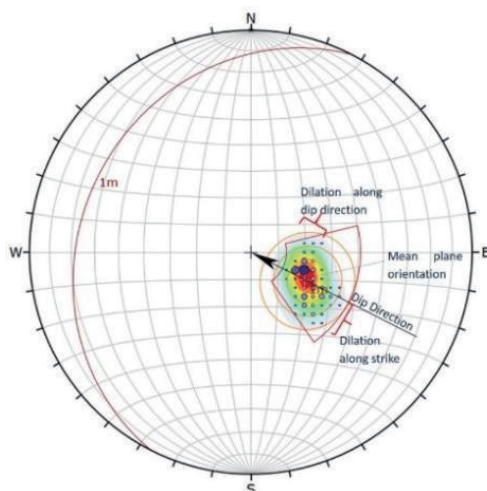


Fig. 8: Stereonet displaying point normal orientations. Overall dip direction indicated by arrow. Variability cones representing 1, 2

and 3 standard deviations displayed in orange. Surface roughness and dilation angle are directionally dependant. To quantify any anisotropy, the dilation angle was defined both along dip direction and along strike for each bedding surface. This was intended to capture whether there was a difference in what the surface would experience between standard planar sliding (down dip) and a situation where applied force of water (from dam spilling) may force a block to travel across the surface (along strike). A pronounced anisotropy was observed, with a mean dilation of 11 degrees along dip direction, and 14 degrees along strike.

4 DATA APPLICATION

The analysis of defect set orientation, spacing and waviness collected through remote sensing allowed for an increased geological understanding of the setting of Bendora Dam, as outlined in companion paper Baxter-Crawford and Stariha (2022). The application of waviness and dilation angle to shear resistance has also been addressed in this companion paper.

5 CONCLUSIONS

The analysis of remote sensing data in the form of point clouds allowed for the assessment of defect set in slopes which were not physically accessible. The program CloudCompare was used to define the orientation, spacing, waviness and dilation angle of three sub-vertical joint sets and a bedding set. Visual aids were applied in the form of segregated and coloured point clouds, assisting in the visualization of the relationship between defect sets and topography. Of particular note was the directional dependence of the dilation angle observed by analysing the normal orientation of each point along a defect plane.

ACKNOWLEDGEMENTS

The authors wish to thank Icon Water for their approval to publish this paper.

REFERENCES

- Baxter-Crawford, H. & Stariha, K. 2022. Collation and Interpretation of structural data at various scales to inform 3D structural models. *10th International Conference on Physical Modelling in Geotechnics*, Daejeon, Korea
- Dong, X., Xu, Q., Huang, R., Liu, Q. & Kieffer, S. 2019. Reconstruction of surficial rock blocks by means of rock structure modelling of 3D TLS point clouds: The 2013 Long-Chang Rockfall. *Rock Mech. Rock Eng.* 53: 671-689
- Gigli, G. and Casagli, N. 2011. Semi-automatic extraction of rock mass structural data from high resolution LIDAR point clouds. *International Journal of Rock Mechanics and Mining Sciences*, 48: 187-198.
- Turner, A. K., Slob, S., & Hack, H. R. 2006. Evaluation, and management of unstable rock slopes by 3D laser scanning. *International Association for Engineering Geology and the Environment*, 1-11.